Pergamon

Pattern Recognition, Vol. 31, No. 2, pp. 181–192, 1998

0031-3203/98 $17.00+.00

PII: S0031-3203(97)00018-6

SKEW-SYMMETRY DETECTION VIA INVARIANT SIGNATURES

A. M. BRUCKSTEIN* and D. SHAKED
Center for Intelligent Systems, Technion, IIT, 32000, Haifa, Israel

(*Received* 4 *June* 1996; *in revised form* 14 *January* 1997)

Abstract—We propose a new approach to skew-symmetry detection, based on the theory of invariant signatures for planar objects. Invariant signatures associated to object boundaries are generalizations of the curvature versus arclength description of curves, invariant under geometric transformations more complex than the Euclidean ones. We show that symmetries of objects, and hence of closed boundaries, translate into simple structures in the invariant signature functions and are therefore, in principle, readily detectable. © 1997 Pattern Recognition Society. Published by Elsevier Science Ltd.

Symmetry Skew-symmetry Invariant signatures Shape analysis

1. INTRODUCTION

Patterns and symmetries are a source of endless enjoyment for all of us: We seek to detect symmetry and pattern whenever we are presented with visual or auditory stimuli and we try to design and produce things with interesting symmetries and structures. H. Weyl in his remarkable book *Symmetry*,[1] shows that "symmetry in its several forms, bilateral, translatory, rotational, ornamental", etc. is a geometric concept closely related to the notion of "invariance of a configuration of elements under a group of automorphic transformations".

Computer Vision and Computational Geometry researchers interested in shape analysis have devoted much work to developing symmetry detection methods, see references (2–5). The algorithms that were developed for symmetry detection exploit in clever ways the invariance of shapes or configurations of geometric elements implied by various types of symmetries.

If we have a bounded configuration of geometric elements (points, lines, basic simple shapes) in 2D, the groups of transformation whose invariances generate symmetries are rotations about the centroid and reflections about lines passing through it. If, furthermore, the number of feature points in the bounded geometric configuration is finite then the size of the group of transformations that could induce symmetry invariances is finite. Hence it is usually not very complicated to detect symmetries in such cases: We must perform a finite number of tests for reflection or for rotation symmetries.

Atallah[4] and Eades[5] have shown that symmetries of planar point configurations consisting of points and segments can be detected with efficient algorithms. For example, detecting reflection symmetry for polygons can be done in the following way: encode the closed polygonal line defined by the (cyclic) sequence of points $\{P_1P_2P_N\}$ via an associated cyclic sequence of triplets, each associated to a break point P_i,

$$(d_N\alpha_1d_1)(d_1\alpha_2d_2)(d_2\alpha_3d_3)\cdots(d_{N-1}\alpha_Nd_N),$$

where d_i is the length of the segment P_iP_{i+1} and α_i is the angle in the range $[-\pi,\pi]$ at the ith vertex. This (obviously redundant) representation clearly enables us to reconstruct the polyline up to a Euclidean transformation, and the various symmetries of the object, if they exist, will become apparent in it. In particular, the reflection symmetry appears as a palindromic structure of the cyclic sequence $\{\cdots d_i\alpha_{i+1}d_{i+1}\cdots\}$ about some center point. This property is easily detected with a linear algorithm in N, see references (4,5).

A related problem of much interest to the Computer Vision community is the detection of "skewed" symmetries. To give an illustrative example, assume that a symmetric planar shape is projected into an image by a pin-hole camera. The image clearly loses its symmetry in the process, whenever the image plane is not parallel to the object plane. However we, humans, are exhibiting remarkable capabilities of detecting symmetries in spite of such viewing distortions. It is considered important to have the capability of analyzing and recognizing shapes and their symmetries, even when those underwent quite severe distortions due to the, generally nonlinear, projection involved in the image acquisition process. Hence, the problem of detecting skew symmetries received a lot of attention in the machine vision literature, see for example the survey of the "state-of-the-art" in a recent paper by Gross and Boult Gross and the references therein. Most of the work in this context, including[6] (and also references (7–9)), dealt with skew symmetries as defined by T. Kanade,[10,11] assuming distortions due to orthographic projections and devising various, most often global and sometimes local and feature-based, ad hoc procedures to determine the slanted symmetry axis of distorted planar objects, with reflexive symmetry. Some of the work in this area was quite clever and elegant. However, it seems to us that a general approach never emerged.

* Author to whom correspondence should be addressed.

In this paper we propose a general framework for symmetry analysis of planar shapes based on the use of invariance theory. Indeed, differential, semi-differential and various types of local invariants were recently proposed for the descriptions of planar shapes that would enable their recognition even in distorted and partially occluded instances. The idea is to use an invariant "signature"-based boundary curve description, generalizing the commonly used curvature versus arclength representation that is invariant only under Euclidean distortions. Through the recent work of several teams of researchers in computer vision, work based on the classical theory of differential and geometric invariants for the affine and projective groups of transformations,[12,13] a wealth of invariant signatures, of "generalized curvatures" versus "invariant arclength" representations are now available. See the papers (14–22).

Invariant arclength was first introduced to model symmetries and other similarities by Van Gool *et al.*[23] The ideas presented in this paper first appeared in reference (24). In a very recent paper[25] Van Gool *et al.* present special invariants for the smallest possible subgroup of transformations characterizing skew symmetries. Those invariants for the affine skew symmetry are simpler than the common affine or equiaffine invariants, however in order to compute them a pair of symmetrically corresponding points has to be given.

The main thesis of this paper is that, symmetries, if present, will always manifest themselves as special structures in the projection-invariant signature functions, thereby reducing the problem of symmetry detection and analysis to that of analyzing a (periodic) 1D function. The computation and analysis of the signatures does not require any initial knowledge or assumption of skew symmetric point matches.

Detection of symmetries of planar shapes affected by the viewing projection that generated their images can be accomplished by encoding the boundaries of the objects in the image in ways that are invariant under those distorting transformations. This invariance implies that the original, undistorted and hence symmetric object (in the real "Euclidean" sense) will have the same description as the entire class of its possible (distorted) images.

Therefore,

> If symmetry in the Euclidean plane implies invariance under some $\mathbb{R}^2 \to \mathbb{R}^2$ transformations, like reflections about some axis passing through the centroid of the shape or rotations by some angles, symmetry of shapes viewed through some distorting, say projective or affine transformation implies invariance under the "conceptual" concatenation of the projection and symmetry transformation maps.

The next section will discuss the problem of detecting reflexive (mirror) symmetry for planar shapes distorted by affine and projective viewing transformations. The reader should realize that the approach is quite general and can be readily carried over to other types of symmetries and different $\mathbb{R}^2 \to \mathbb{R}^2$ distorting maps. In Section 3, we discuss the easier case of planar polygons and develop methods for reflexive symmetry detection under affine and projective transformations. In Section 4, we dwell upon some practical considerations arising in the application of the proposed method to polygonal shapes. Those considerations are readily carried over to the case of general shapes. Next we present simulation results in Section 5, and conclude in Section 6.

2. GENERAL APPROACH TO SKEW SYMMETRY DETECTION

A planar object with reflexive or mirror symmetry has a boundary curve $\mathscr{C}(s)$ with a (periodic) curvature versus arclength description $K(s)$ that clearly displays the symmetry: There are two points $\mathscr{C}(p_1)$, $\mathscr{C}(p_2)$ on the curve such that

$$K(p_i + s) = K(p_i - s) \quad \text{for } i \in \{1, 2\}.$$

Hence mirror symmetry induces a palindromic structure on the $K(s)$ representation. Conversely, if $K(s)$ has this structure the curve we can reconstruct from it (uniquely, up to a Euclidean transformation) will necessarily be mirror symmetric. Thus the $K(s)$ representation elegantly solves the problem of mirror symmetry detection for shapes whose instances are "distorted" by Euclidean and even similarity transformations in the plane.

Suppose however that we pose the following general question: Given a shape S and a continuous group of plane transformations $\mathscr{T}_\theta : \mathbb{R}^2 \to \mathbb{R}^2$ (parameterized by θ) that distort the shape, how could we detect whether the "original" undistorted shape is mirror-symmetric given a distorted instance of S, i.e. $\mathscr{T}_{\theta_0}[S]$.

The answer to this question is the following: Suppose that we can find a $\mathscr{T}$-invariant metric on the planar curve (like the Euclidean-invariant arclength metric) and furthermore assume we can find a signature function (like the Euclidean curvature) that is also $\mathscr{T}$-invariant. Such invariant metrics and signatures will be based on some local, differential or geometric properties of the curve. Denote the signature versus the $\mathscr{T}$-invariant arclength function by $\rho(\tau)$. All $\mathscr{T}_\theta$-transformed versions of S will then have the same $\rho(\tau)$ modulo some initialization for the (clockwise) traversal of the boundary curve. (The initialization clearly induces a shift in τ; $\tau \to \tau - \tau_0$).

Since the identity transformation always belongs to the group $\mathscr{T}_\theta$, the original, truly symmetric, instance of S will have the same $\rho(\tau)$. But $\rho(\tau)$ is computed based on some local, geometric properties of the boundary [see references (18–22)], therefore the $\rho(\tau)$ description of a mirror symmetric S will exhibit the same type of palindromic symmetry like $K(s)$ for the Euclidean-invariant case.

Therefore, the problem of symmetry detection under the distorting $\mathscr{T}$-transformation is quite elegantly solved if a $\mathscr{T}$-invariant signature versus $\mathscr{T}$-invariant arclength is found. This signature should have the property that from it the boundary is uniquely determined up to a transformation $\mathscr{T}$, [i.e. the equivalence class of all shapes that are

$\mathcal{T}$-distortions of each other is uniquely characterized by $\rho(\tau)$].

As we shall see in the sequel, for planar polygons, such signatures are readily found for the groups of affine and projective transformations.

In case we deal with continuous curves, the classical theory of differential invariants yields signatures with the desired property, however, those are unfortunately based on using high derivatives of the parameterized curve representations.[12,13,15,17] Several approaches have been developed to circumvent the need for high derivatives, through the use of global point matches,[18,19,22] via local frames,[21] or by the local use of global invariants in conjunction with finite differences w.r.t the $\mathcal{T}$-invariant arclength.[20]

3. SKEW SYMMETRY DETECTION FOR PLANAR POLYGONS

In this section we discuss the case of polygonal curves. This easier case has some unique properties as for example the need for *two* independent signature functions associated to a readily available discrete arclength parameterization: A sequential numbering of the polygon vertices. In the following two subsections we present detailed solutions for the detection of affine and projective skew symmetric polygons.

Suppose we are given a planar polygon defined via its sequence of vertices $\mathbf{Q}=\{Q_1, Q_2 Q_N\}$ and we wish to determine whether it can be the image of a mirror-symmetric polygon. If a closed polygonal curve $\mathbf{P}=\{P_1 P_2 P_N\}$ undergoes a transformation the vertices P_i will be mapped into the vertices Q_i of the resulting $\mathcal{T}$ transformed image $\mathbf{Q}$. Clearly the ordered sequencing of the vertices readily acts as an invariant "arclength" parameterization. We now ask ourselves what type of invariant signatures we could associate to each vertex of the polygonal curve. Recall that we need to produce a signature sequence associated with $\mathbf{Q}$ (that by invariance will be the same as the one computed for $\mathbf{P}$) enabling the *unique reconstruction* of the equivalence class of all planar polygonal curves that are $\mathcal{T}$-equivalent to $\mathbf{P}$.

Suppose we have a single invariant quantity, ρ, associated with every vertex of the polygon. It is easy to see that the scalar invariant series $\{\rho(i)\}$, in conjunction with any initialization involving a finite number of vertices is not sufficient to reconstruct the entire polygon up to an arbitrary transformation. (Just like the sequence of edge-length is a valid Euclidean-invariant signature but is clearly insufficient for reconstruction of the shape—although it might be good enough for model-based recognition.) A single invariant descriptor restricts the vertex to a one-dimensional locus in the plane because it constitutes only one constraint on the vertex which would otherwise have two degrees of freedom in the plane. We conclude that we need two independent invariant quantities associated to each vertex. In a sense we see that the invariant arc length description provided by the order of the vertices did not help us to get by the need to find two independent invariant descriptions for the curve.

In the following subsections we suggest appropriate invariants for the affine and projective groups of transformations. For each transformation we suggest two symmetrically defined invariants ρ^{L}, and ρ^{R}. We further present a polygon reconstruction procedure for each pair of invariants, and show how to reconstruct a truly symmetric instance from a given palindromic sequence. We separate two generic cases of palindromic sequences:

- *Vertex symmetric* sequences palindromic about, say the ith element obey

$$\rho^{\mathrm{R}}(i-k)=\rho^{\mathrm{L}}(i+k), \rho^{\mathrm{L}}(i-k)=\rho^{\mathrm{R}}(i+k).$$

- *Edge symmetric* sequences palindromic about the space between elements i and $i-1$ obey

$$\rho^{\mathrm{R}}(i-k-1)=\rho^{\mathrm{L}}(i+k), \rho^{\mathrm{L}}(i-k-1)=\rho^{\mathrm{R}}(i+k).$$

3.1. *Affine skew symmetry*

The affine group of transformations $\mathcal{T}_a : \mathbb{R}^2 \to \mathbb{R}^2$ is given by

$$[x', y'] = [x, y]A + [t_x, t_y],$$

where A is an invertible matrix. The affine group of transformations has six degrees of freedom: Two in the translation vector and four in the matrix A. Any 2×2 invertible matrix A can be multiplicatively decomposed as follows:

$$A = R \cdot D \cdot S = \begin{bmatrix} \cos\phi & \sin\phi \\ -\sin\phi & \cos\phi \end{bmatrix} \begin{bmatrix} a_x & 0 \\ 0 & a_y \end{bmatrix} \begin{bmatrix} 1 & s \\ 0 & 1 \end{bmatrix}, \tag{1}$$

where R is a unitary (rotation) matrix, D a diagonal matrix, and S an upper triangular (skew) matrix. In this decomposition ϕ is the rotation parameter, a_x and a_y the scale parameters in the x and y directions respectively, and s the skew parameter.

It is well known that $\mathcal{T}_a$ preserves area-ratios, since under $\mathcal{T}_a$ areas of shapes are uniformly scaled by $|\det A| = a_x \cdot a_y$. The signature sequence $\{\rho(1), \rho(2), \ldots, \rho(N)\}$ associated to $\mathbf{Q} = \{Q_1, Q_2, \ldots, Q_N\}$ should therefore be (functions of) area ratios of various shapes "anchored" at successive vertices of Q.

For example, we could define

$$\rho^1(i) = \frac{\|\Delta(Q_{i-1}, Q_i, Q_{i+1})\|}{\|\Delta(Q_{i-2}, Q_i, Q_{i+2})\|} \tag{2}$$

or

$$\rho^2(i) = \frac{\|\Delta(Q_{i-2}, Q_{i-1}, Q_i)\|}{\|\Delta(Q_i, Q_{i+1}, Q_{i+2})\|}. \tag{3}$$

In the above $\|\Delta(A, B, C)\|$ denotes the area of the triangle $\Delta(A, B, C)$ [see Fig. 1(a)]. Alternatively, we can use the (invariantly defined) segment intersections q_i^{L}, q_i^{R} [see Fig. 1(b)] to define a symmetric pair of invariants:

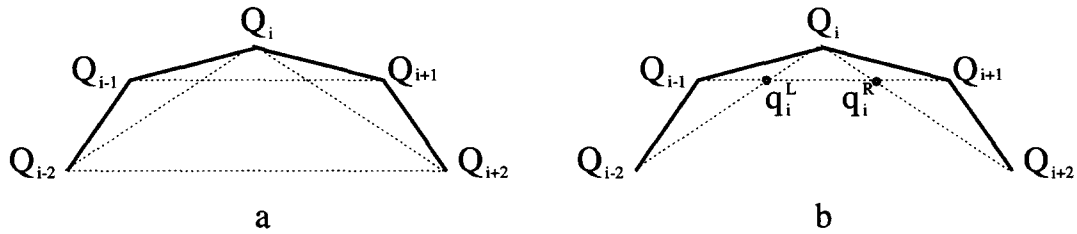

Fig. 1. Two affine invariants for polygons.

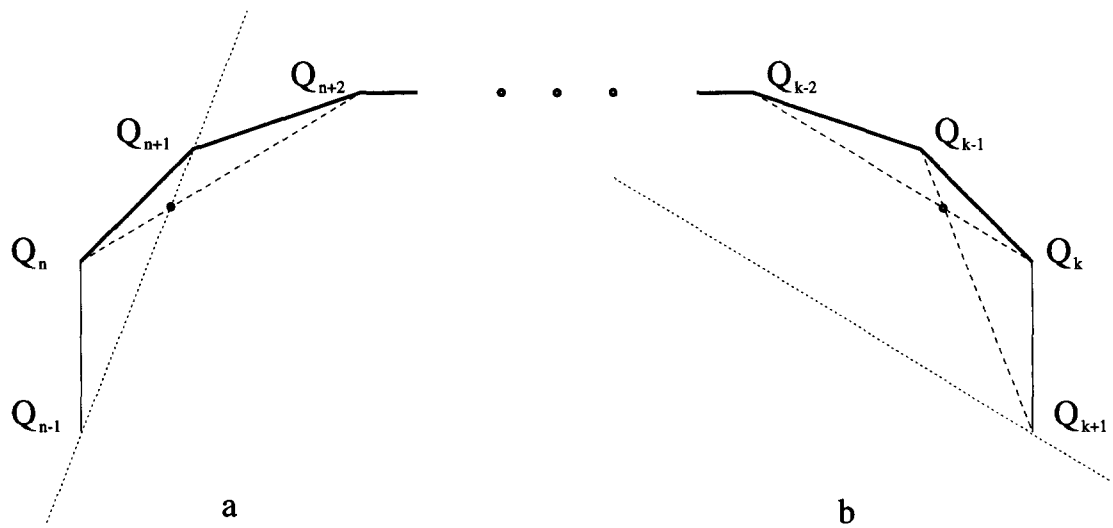

Fig. 2. A single affine invariant ρ^{L} is not sufficient for reconstruction.

$$\rho^{L}(i)=\frac{\|\Delta(q_i^{L},Q_{i-1},Q_i)\|}{\|\Delta(Q_{i-1},Q_i,Q_{i+1})\|},\ \rho^{R}(i)=\frac{\|\Delta(Q_i,Q_{i+1},q_i^{R})\|}{\|\Delta(Q_{i-1},Q_i,Q_{i+1})\|}. \tag{4}$$

Here we have

$$\rho^{L}(i)=\frac{\|(q_i^{L},Q_{i-1})\|}{\|(Q_{i-1},Q_{i+1})\|},\ \rho^{R}(i)=\frac{\|(Q_{i+1},q_i^{R})\|}{\|(Q_{i-1},Q_{i+1})\|}, \tag{5}$$

where $\|(A,B)\|$ denotes the length of the line segment from A to B. Similar types of invariants were proposed for affine invariant recognition of polygons under occlusion.[26]

Assume the position of a finite number of consecutive vertices $Q_n,\ldots,Q_k$ is given. It is easy to see that from a given invariant series $\{\rho^{L}(i)\}$ we can constrain vertex Q_{n-1} to a line trough (the given) Q_{n+1}, whose azimuth is determined by $\rho^{L}(n+1)$ [see Fig. 2(a)]. Similarly the location of Q_{k+1} can be constrained to a line parallel to the segment through (the given vertices) Q_{k-2} and Q_k, whose distance from the former is determined by $\rho^{L}(k)$ [see Fig. 2(b)]. To fix the locations of Q_{n-1} and Q_{k+1} we have to use the invariant series $\{\rho^{R}(i)\}$. Clearly, the constraints imposed by $\{\rho^{R}(i)\}$ on the vertices are symmetric to the constraints of $\{\rho^{L}(i)\}$. It is easy to see that the constraints are not independent only if three consecutive vertices (e.g. Q_n, Q_{n+1}, and Q_{n+2}) are located on a straight line.

Since the affine transformation group has six degrees of freedom, at least six values must be set by the initial conditions to enable reconstruction of the polyline. Indeed, it is possible to reconstruct the polygon from $\{\rho^{L}(i)\}$, $\{\rho^{R}(i)\}$ and three consecutive vertex locations given as an initial condition. Different positions of the initial conditions result in various affine transformations of the reconstructed polygon.

Next we shall show, in a constructive manner, that a joint palindromic structure of $\{\rho^{L}(i)\}$ and $\{\rho^{R}(i)\}$ is sufficient to determine affine skew symmetry. We do that by reconstructing a mirror-symmetric affine transformation of the given polygon. Note that an affine transformation of a symmetric shape whose symmetry axis is aligned with either the x axis or the y axis, loses its symmetry property only if the skew parameter is nonzero. Hence, specifying an initial condition for a symmetric shape will "cost" us only one degree of freedom (i.e will set the skew to zero).

If the sequence of invariants is vertex symmetric about its ith element, then an isosceles triangle initial condition $\|(Q_{i-1}Q_i)\|=\|(Q_iQ_{i+1})\|$ will cause the reconstructed polygon to be mirror symmetric, see Fig. 3(a). Changing the position of the initial triangle will translate the reconstructed polygon. Rotating the initial condition around Q_i will rotate it. Changing the height of the isosceles triangle or its width, will scale the polygon in directions parallel or perpendicular to the symmetry

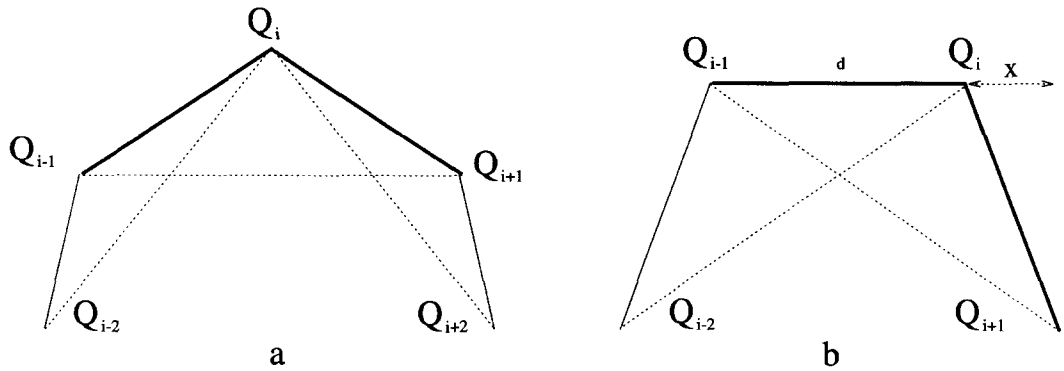

Fig. 3. Initial conditions causing a symmetric reconstruction from affine invariants.

axis. Altogether these variations account for the five degrees of freedom remaining after the skew was set to zero.

If the sequence of invariants is edge symmetric about the space between elements i and $i-1$, and an initial condition is given by Q_{i-1}, Q_i, Q_{i+1}: Changing the position of the initial triangle and rotating it, will translate the reconstructed polygon and rotate it accordingly. Scaling the initial condition parallel (perpendicular) to the direction $Q_{i-1}Q_i$, will scale the polygon perpendicular (parallel) to the symmetry axis. The only degree of freedom left is the position of Q_{i+1} on a line parallel to $Q_{i-1}Q_i$ [see Fig. 3(b)]. Since $\rho^{\mathrm{R}}(i-1)=\rho^{\mathrm{L}}(i) \triangleq \lambda$ it may be shown that Q_{i-2} is on the same line parallel to $Q_{i-1}Q_i$ as Q_{i+1}, and its horizontal distance from Q_{i+1} is $[d(1-\lambda)/\lambda]-x$, where d is the length of the edge $Q_{i-1}Q_i$ and x is the horizontal distance between Q_i and Q_{i+1}, see Fig. 3. Clearly, selecting the last degree of freedom so that $[d(1-\lambda)/\lambda]=d+2x$, i.e. $x=[d(1-2\lambda)/2\lambda]$ causes Q_{i-2} to be symmetric to Q_{i+1}, and the rest of the reconstruction is naturally symmetric as well. Selecting another x, would cause the reconstruction to be skewed.

3.2. *Projective skew symmetry*

The projective group of transformations $\mathscr{T}_p : \mathbb{R}^2 \to \mathbb{R}^2$ is given by

$$[x', y'] = \frac{1}{1 + w_x x + w_y y}[x, y]A + [t_x, t_y],$$

with A an invertible matrix. The projective group of transformations has eight degrees of freedom: Two in the translation vector, four in the matrix A, and two tilt parameters $w_x = \partial H/\partial x$, and $w_y = \partial H/\partial y$, indicating the tilt of the object plane H in the camera coordinate system. As in the affine case the four degrees of freedom in the invertible matrix A can be assigned to ϕ the rotation, a_x and a_y the scales in the x and y directions, and s the skew parameter. It is well known that $\mathscr{T}_p$ preserves cross-ratios. The cross-ratio is defined for four collinear points P_1, P_2, P_3, P_4 ordered on a line.

$$\mathrm{CR}(P_1, P_2, P_3, P_4) = \frac{\|(P_1, P_3)\| \cdot \|(P_2, P_4)\|}{\|(P_1, P_4)\| \cdot \|(P_2, P_3)\|}.$$

$\mathscr{T}_p$ also preserves line intersections. The signature sequence $\{\varphi(1), \varphi(2), \ldots, \varphi(N)\}$ associated to $\mathbf{Q}=\{Q_1, Q_2, \ldots, Q_N\}$ should therefore be based on cross-ratios of collinear points anchored at either the vertices of $\mathbf{Q}$ or intersections of lines through the vertices.

For example we could define $\varphi(i)$ to be the cross-ratio of Q_{i-1}, C_i^{L}, C_i^{R}, and Q_{i+1}, where C_i^{L} and C_i^{R} are the intersections of the line through Q_{i-1}, Q_{i+1}, with the lines through Q_i, Q_{i+2} and Q_i, Q_{i-2} respectively, see Fig. 4(a).

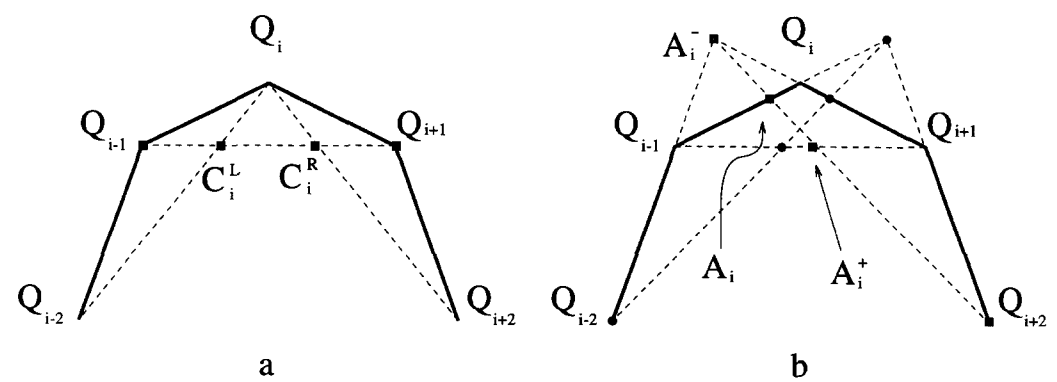

Fig. 4. Possible projective invariants for polygons.

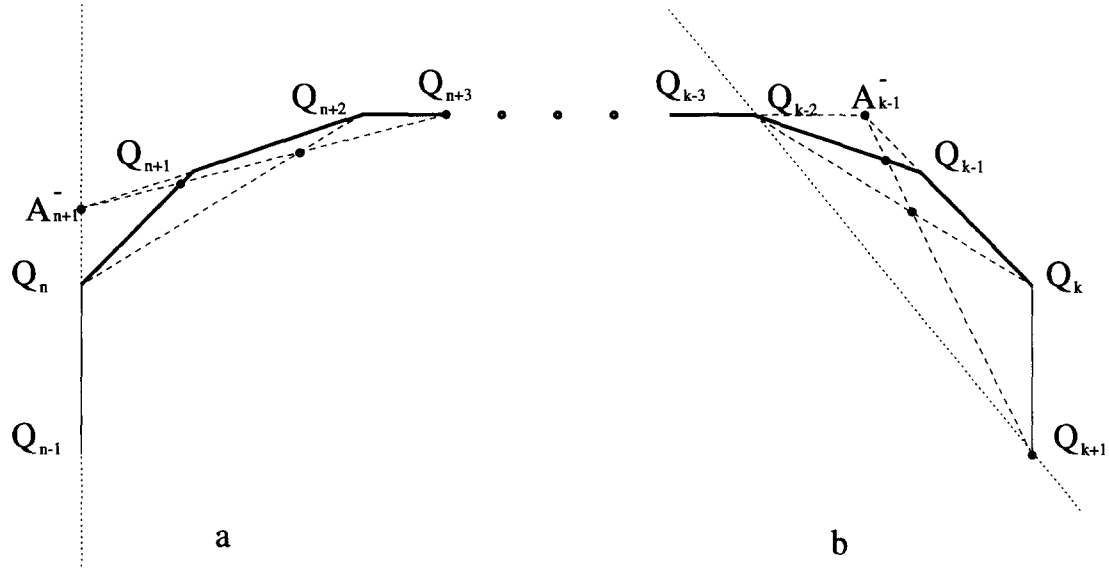

Fig. 5. A single projective invariant φ^{L} is not sufficient for reconstruction.

In order to maintain left–right symmetry in the invariant pair, we use the projective invariants φ^{L} and φ^{R}. φ^{L} is the cross-ratio of A_i^-, A_i, A_i^+, and Q_{i+2}. A_i^- is the intersections of the line through Q_{i-2}, Q_{i-1} with the line through Q_{i+1}, Q_i, and A_i, A_i^+ are the intersections of the line through A_i^-, Q_{i+2}, with the lines through Q_{i-1}, Q_i and Q_{i-1}, Q_{i+1} respectively. The definition for φ^{R} is similar. In Fig. 4(b) $\varphi^{L}(i)$ is the cross-ratio of points denoted by square bullets, and $\varphi^{R}(i)$ the cross-ratio of points denoted by circular bullets.

Assume the position of a finite number of consecutive vertices $Q_n, \ldots, Q_k$ is given. Considering $\varphi^{L}(n+1)$ we note that since the location of Q_{n-1} is not yet determined, the location of A_{n+1}^- also cannot be defined. Remember now that the cross-ratio is identical for all point quadruples created by the intersection of a pencil of four lines with another line. Note that $\varphi^{L}(n+1)$ is the cross-ratio of the intersection points of the line through A_{n+1}^-, Q_{n+3} with the pencil from Q_n to Q_{n+3}, Q_{n+2}, Q_{n+1}, and A_{n+1}^-. Since the cross-ratio is invariant to the line crossing the pencil, the location of A_{n+1}^- and hence also Q_{n-1} can be confined to a line through Q_n, whose azimuth is determined by $\varphi^{L}(n+1)$, see the dotted line in Fig. 5(a). Similar arguments are valid for the reconstruction from the other side of the initial condition, the dotted line through Q_{k-2} being the constraint induced by φ^{L} on the location of Q_{k+1}, see Fig. 5(b). Clearly, the constraints imposed by $\{\varphi^{R}(i)\}$ on the vertices are symmetric to the constraints of $\{\varphi^{L}(i)\}$. φ^{L} and φ^{R} are not independent only in cases where they get extreme values, e.g. if Q_{n-1} is located on the line through Q_n and Q_{n+2}. In these cases, the values of the invariants are extremely sensitive to the location of the vertices, and hence offer little information in any practical application. In Section 4, we describe a way to recognize such situations and ignore them in the detection process.

Since the projective transformation group has eight degrees of freedom, at least eight numbers are necessary as initial conditions for the reconstruction. Indeed it is possible to reconstruct the polygon from $\{\varphi^{L}(i)\}$, $\{\varphi^{R}(i)\}$ and four consecutive point locations provided as initial conditions. Different positions of the initial conditions result in different projective transformations of the reconstructed polygon.

Next we show, in a constructive manner, that a joint palindromic structure of $\{\varphi^{L}(i)\}$ and $\{\varphi^{R}(i)\}$ is sufficient to determine projective skew symmetry. We will do that by reconstructing a mirror-symmetric projective transform of the given polygon. Note that a projective transformation of a symmetric shape whose symmetry axis is aligned with the y axis, loses its symmetry property only if either the skew or the x-tilt parameter w_x are non-zero. Specifying an initial condition for a symmetric shape will "cost" here two degrees of freedom.

If the sequence of invariants is edge symmetric about the space between elements i and $i-1$, then a symmetric trapezoid initial condition as in Fig. 6(a) will cause the reconstructed polygon to be symmetric. Changing the position of the initial configuration will translate the reconstructed polygon. Rotating the initial condition will rotate it. Scaling the configuration in the symmetry axis direction or perpendicular to it, will scale the reconstructed polygon accordingly. Changing the relative size of the trapezoid bases accounts for tilting the object plane in the symmetry axis direction. Altogether these variations account for the six remaining degrees of freedom.

Suppose the sequence of invariants is vertex symmetric about the ith element, and an initial condition is given by Q_{i-1}, Q_i, Q_{i+1}, Q_{i+2}, with $\Delta(Q_{i-1}, Q_i, Q_{i+1})$ an isosceles triangle as in Fig. 6(b). We want to show that we can find the symmetry inducing initial condition by sliding Q_{i+2} on a line parallel to the line through Q_{i-1}, Q_{i+1}, see Fig. 6(b). Denote the position of Q_{i+2} on the parallel line by x. It is possible to show that for a symmetric position of Q_{i-2}, $\varphi_i^{L}(x)=\varphi_i^{R}(x)$ is a one-to-

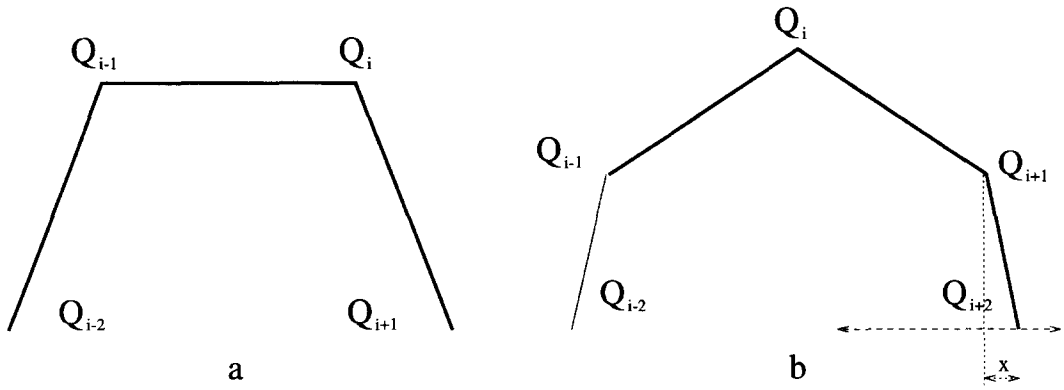

Fig. 6. Initial conditions causing a symmetric reconstruction from projective invariants.

one function. Thus, for every given $\varphi_i^L=\varphi_i^R$ there is a unique x which causes Q_{i-2} to be symmetric to Q_{i+2}, which provides a symmetric initialization for a fully symmetric polygon. Here also we can account for the six degrees of freedom in the translation, rotation, in-axis scaling, and off-axis scaling of the initial condition. The last degree of freedom is the ratio between the height of the isosceles triangle and the distance between Q_{i+2} and the line through Q_{i-1}, Q_{i+1}.

4. PRACTICAL CONSIDERATIONS

In this section we discuss a few practical issues. We naturally consider issues relevant to polygonal curves, however the problems we present as well as the solutions we propose are valid also for general curve descriptions.

How is the symmetry reflected in the invariants? If a shape is symmetric, there are two points $\mathscr{C}(p_1)$, $\mathscr{C}(p_2)$ where the symmetry axis crosses the boundary, and around which the invariant signature is symmetric $\rho(p_i+p) \sim \rho(p_i-p)$. The symmetry axis of polygonal shapes can cross their boundary either at a vertex or at the middle of an edge. We distinguish the two cases as vertex symmetry and edge symmetry. As already mentioned, to establish symmetry of polygonal shapes we need two independent signature functions. We use a symmetrically defined pair of signatures: the symmetry of the signatures is a reflexive symmetry of their geometrical interpretations, e.g. ρ_L and ρ^R (4) in Fig. 1(b), or φ^L and φ^R in Fig. 4(b). Thus vertex symmetric signatures palindromic about the ith vertex obey

$$\rho^R(i-k)=\rho^L(i+k), \quad \rho^L(i-k)=\rho^R(i+k) \tag{6}$$

and edge symmetric signatures palindromic about the edge between vertices i and $i-1$ obey

$$\rho^R(i-k-1)=\rho^L(i+k), \quad \rho^L(i-k-1)=\rho^R(i+k). \tag{7}$$

If for polygonal curves we do not chose a symmetrically defined pair of invariant signatures the symmetry conditions are a little different. A reflexive symmetric invariant [e.g. ρ^1 in equation (2) of a vertex symmetric polygon, obeys $\rho^1(i-k)=\rho^1(i+k)$. Non-symmetric invariants [e.g. ρ^2 in equation (3)], do not always facilitate symmetry detection. In some cases it is possible to find some function F that finds the reflexive symmetric invariant given a sequence of invariants. Then the signature of a vertex symmetric polygon obeys

$$\rho^2(i-k)=F(\rho(i+k-N),\ldots,\rho^2(i+k),\ldots,\rho(i+k+N)). \tag{8}$$

For example for ρ^2 in equation (3), $F(\ldots)=1/\rho(i+k)$, and for ρ^L in equation (4) $F(\ldots)=1-\rho(i+k+2)$.

The above discussion is valid for general curves as well. The curvature, for example, is a symmetric feature, and its first derivative is a non-symmetric feature (the reflexive symmetric feature of the first derivative is trivially its negative).

How are skew symmetric shapes detected? A shape is skew symmetric if we find a good candidate for symmetry axis. A symmetry axis obeys one of equations (6) and (7) or, for some general invariants [equation (8)]. Practically however because of noise and finite accuracy, none of the equations is fully obeyed, and we have to define a measure $E(i)$ for the deviation from symmetry for each vertex i. In our simulations, we chose $E(i)$ to be the maximal absolute difference over all possible values of k. For example, the vertex symmetry indicator equation (6) is

$$E(i)=\max_k\{|\rho^R(i-k)-\rho^L(i+k)|, |\rho^L(i-k)-\rho^R(i+k)|\}.$$

This indicator is simultaneously the l^∞ norm and an order statistics. One can choose any other metric or order statistics, though one has to consider the consequences. For example, an l^2 norm of a large shape may accommodate small deviations from symmetry, and the median statistics may allow drastic local deviations.

The actual decision of whether a specific indicator is sufficiently small to indicate a skew symmetry axis is very difficult to resolve and is, at least partly, connected to the theory of hypothesis testing. In order to compensate for noise in the image, indicators are compared to the

manifestation of the same noise in other indicators obtained for the same shape. The indicators of true symmetry axes are thus expected to have significantly lower values than all the other indicators. Note the we implicitly assumed that shapes are not circle like shapes (in which case it may have been better to chose an absolute threshold on the indicators).

Setting the value of the critical parameter in our implementation, namely, how low should the lowest indicator be to be considered significant (as well as many other possible parameters, e.g. multiple symmetry axes), is purely a hypothesis testing problem. One has to consider the trade of between false alarm (detection of a false symmetry axis) and miss detection (an actual axis not detected). The results presented in the next section indicate that this trade off may be satisfactorily resolved.

What is the sensitivity to noise in the boundary description? Line intersections, characterizing the affine and projective signatures, may sometimes be extremely sensitive features, see, e.g., references (27,28). Places must therefore be located for which the geometry of the (transformed) polygon indicates that small changes in vertex locations may cause large changes in signature values. The weight of errors induced by sensitive signature values is then diminished.

We locate sensitive invariants according to a linear estimation of the (vertex to signature) error gain factor. An error in a signature pair is then weighted so as to indicate the implied error in vertex locations.

$$|\rho^{R}(i-k)-\rho^{L}(i+k)| \rightarrow \frac{|\rho^{R}(i-k)-\rho^{L}(i+k)|}{G_{\rho^{R}}(i)+G_{\rho^{L}}(i)},$$

where $G_{\rho^{R}}(i)$ is the gain factor from errors in vertex locations to (the maximal) error in $\rho^{R}(i)$.

In the simulations we found that such a weighting is necessary in order to obtain robust symmetry indicators. A similar weighting would have to be considered for signatures of general shapes as well.

We have to stress a distinction between two similar but different issues. A shape that is almost symmetric may be *modeled* by a strong boundary noise, however its detection may be more difficult than the detection of a truly skew symmetric shape. Since the invariants have strong non-linearities it would be necessary to devise more sophisticated weighting techniques to cope with the strong boundary noise. Above that, as already mentioned, a different error metric would have to be considered.

Can invariant signatures be used to detect partly occluded skew symmetric shapes? Signatures of partly occluded skew symmetric shapes clearly have segments of symmetric signature sequences. The converse is however not true. Segments of symmetric signature sequences may also occur if for example two symmetric boundary parts undergo different affine or projective transformations, see Fig. 7(a). For fully symmetric

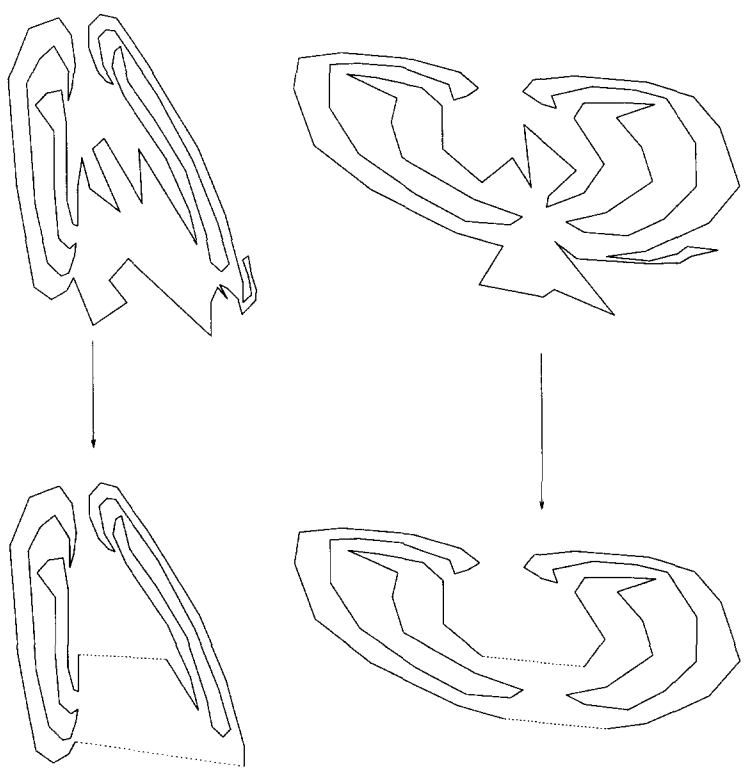

Fig. 7. Symmetric signature subsequences may result from differently skewed boundary segments (a), or from occlusions of a truly symmetric shape (b).

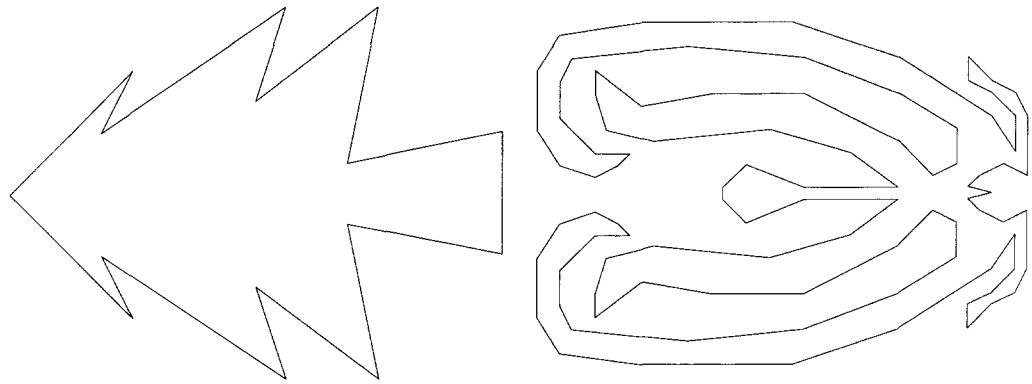

Fig. 8. Original symmetric polygons: (a) tree, (b) flower.

shapes we have shown that the converse is true. To detect skew symmetry under occlusion one has to

1. Locate segments of symmetric signature sequences.
2. Delete all vertices not in those sequences.
3. Connect the corresponding ends of the remaining sequences by straight line segments (dotted lines in Fig. 7).
4. The occluded shape is skew symmetric if and only if the resulting shape is skew symmetric, see Fig. 7. Note that in order to determine that, the invariant signatures of the resulting shapes must be re-calculated.

What are the drawbacks of the specific application for polygonal shapes? The most significant drawback of this application is that truly symmetric polygonal shapes do usually not exist. Polygonal versions of skew symmetric shapes will not do, because the location (and even the number) of the vertices cannot be made symmetric. The polygonal case is mainly interesting because it provides a good and simple example of skew symmetry detection by invariant signatures. Furthermore, all the practical considerations presented in this section remain valid for general shape descriptions.

5. RESULTS

We have checked the proposed symmetry detection scheme for two symmetric polygons, shown in Fig. 8. The polygons were distorted by applying several affine and projective transformations (see Figs 9 and 10, respectively). For each of the 12 polygons presented in these figures, we calculated two affine invariant signature sequences $\{\rho^{L}(i), \rho^{R}(i)\}$ and two projective invariant signature sequences $\{\varphi^{L}(i), \varphi^{R}(i)\}$.

All the 12 polygons in Figs 9 and 10 are projective skew symmetric. The range of projective symmetry indicator values for the true symmetry axis (over all

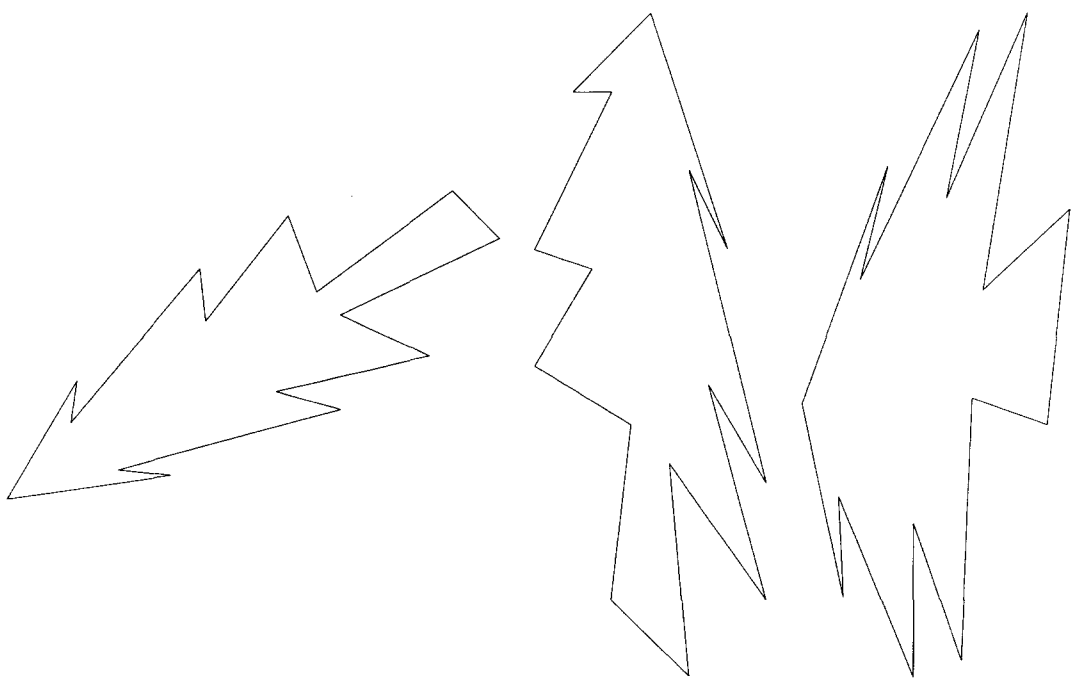

Fig. 9. Affine skew transformations of the tree (a)–(c), and of the flower (d)–(f).

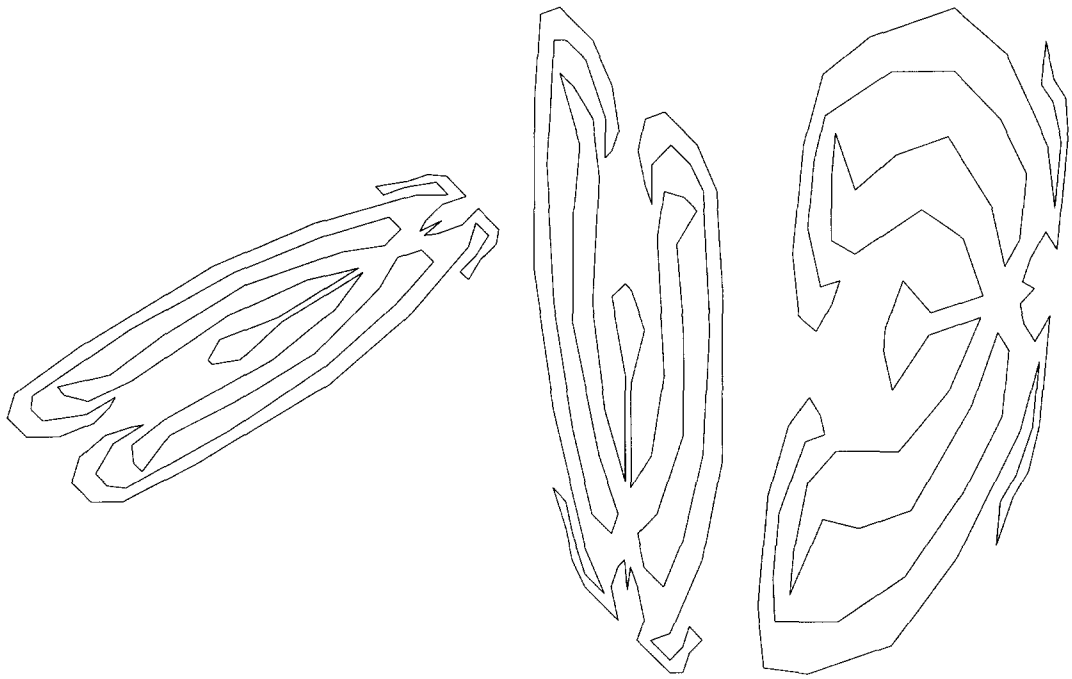

Fig. 9. (Continued).

the 12 images) was 2×10^{-17}–8×10^{-6}. The range of projective symmetry indicator values over all the other (false) vertex symmetry assumptions, and all the 12 polygons was 2×10^{-4}–0.2 We note that for each polygon considered individually, the results were always sharper than may appear from the above cumulative results. The ratio of the indicator value of the true axis to the smallest false indicator value was always less than 10^{-3}, while the range of false symmetry indicator values was never more than 1:100.

The range of affine symmetry indicator values for the true symmetry axis (over all the six affinely distorted

Fig. 10. Projective skew transformations of the tree (a)–(c), and of the flower (d)–(f).

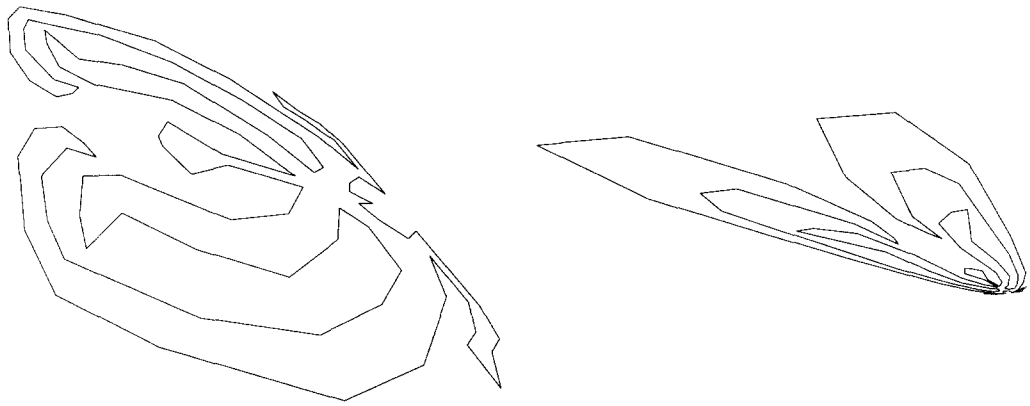

Fig. 10. (Continued).

Table 1. Range of symmetry indicators

Transformation	Affine	Projective
True symmetry axes	6×10^{-16}–4×10^{-14}	2×10^{-17}–8×10^{-6}
False assumptions	0.2–6	2×10^{-4}–0.2

polygons) was 6×10^{-16}–4×10^{-14}, while the range of the indicator values of all the other (false) vertex symmetry assumptions was 0.2–6. These results are summarized in Table 1.

6. CONCLUDING REMARKS

We have presented a general framework for skew-symmetry detection, based on invariant planar curve descriptions. The message of the general theory is that detection of skew symmetry is a process of detecting invariance under a concatenation of two transformations: One characterizing the symmetry sought after and the second, a viewing distortion. We have applied this theory to mirror symmetric polygons distorted by affine and projective viewing transformations. Other types of symmetries can be similarly dealt with, as well as other types of $\mathbb{R}^2 \rightarrow \mathbb{R}^2$ distortions. The theory readily carries over to objects with curved boundaries. This topic is currently under further investigation.

REFERENCES

1. H. Weyl, *Symmetry*. Princeton University Press, Princeton, New Jersey (1952).
2. H. Zabrodsky, Computational aspects of pattern characterization—Continuous symmetry, Ph.D. Thesis, Hebrew University, Jerusalem (1993).
3. S. K. Parmi and D. D. Majunder, Symmetry analysis by computer, *Pattern Recognition* **16**, 63–67 (1983).
4. M. J. Atallah, On symmetry detection, *IEEE Trans. Comput.* **C-34**, 663–666 (1985).
5. P. Eades, Symmetry finding algorithms, in *Computational Morphology*, G. T. Toussiant, ed., pp. 41–51. Elsevier, North-Holland, Amsterdam (1988).
6. A. D. Gross and T. E. Boult, Analyzing skewed symmetries, *Int. J. Comput. Vision* **13**, 91–111 (1994).
7. J. Ponce, On characterizing ribbons and finding skewed symmetries, *CVGIP* **52**, 328–340 (1990).
8. T. J. Cham and R. Cipolla, A local approach to recovering global skewed symmetry, *Proc. Twelfth ICPR*, Jerusalem, pp. 222–226 (1994).
9. R. Glachet, J. T. Lapreste and M. Dhome, Locating and modeling a flat symmetric object from a single perspective image, *CVGIP: Image Understanding* **57**, 219–226 (1993).
10. T. Kanade, Recovery of the 3D-shape of an object from a single view, *Artif. Intell.* **17**, 409–460 (1981).
11. T. Kanade and J. R. Kender, Mapping image properties into shape constraints: Skewed symmetry, affine transformable patterns, and the shape-from-texture paradigm, in *Human and Machine Vision*, J. Beck, B. Hope and A. Rosenfeld, eds, pp. 237–257. Academic Press, New York (1983).
12. S. Buchin, *Affine Differential Geometry*. Science Press, Beijing, China (1983); Gordon and Breach Science Publishers, New York (1981).
13. E. P. Lane, *A Treatise on Projective Differential Geometry*. University of Chicago Press, Chicago (1941).
14. D. Cyganski, J. A. Orr, T. A. Cott and R. J. Dodson, An affine transform invariant curvature function, *Proc. First ICCV*, London, pp. 496–500 (1987).
15. I. Weiss, Projective invariants of shapes, Center for Automation Research Report, CAR-TR-339 (January 1988).
16. K. Arbter, W. E. Snyder, H. Burkhardt and G. Hirzinger, Application of affine invariant Fourier descriptors to recognition of 3D objects, *IEEE Trans. PAMI* **1**(7), 640–647 (July 1990).
17. A. M. Bruckstein and A. N. Netravali, On differential invariants of planar curves and the recognition of partially occluded planar shapes, *Visual Form Workshop*, Capri (1991).
18. L. Van Gool, T. Moons, E. Pauwels and A. Oosterlinck, Semi-differential invariants, *DARPA/ESPRIT Workshop on Invariants*, Reykjavik, Iceland (March 1991).
19. E. B. Barrett, P. Payton and M. H. Brill, Contributions to the theory of projective invariants for curves in two and three dimensions, *DARPA/ESPRIT Workshop on Invariants*, Reykjavik, Iceland (March 1991).
20. A. M. Bruckstein, R. J. Holt, A. N. Netravali and T. J. Richardson, Invariant signatures for planar shape recognition under partial occlusion, *CVGIP: Image Understanding* **58**(1), 49–65 (July 1993).
21. I. Weiss, Noise resistant invariants of curves, *IEEE Trans. PAMI* **15**, 943–948 (September 1993).
22. T. Moons, E. J. Pauwels, L. Van Gool and A. Oosterlinck, Foundations of semi-differential invariants, *Int. J. Comput. Vision* **14**, 25–47 (1995).

23. L. Van Gool, J. Wagemans, J. Vandeneede and A. Oosterlinck, Similarity extraction and modeling, *Proc. ICCV 90*, pp. 530–534 (1990).
24. A. M. Bruckstein and D. Shaked, Skew symmetry detection via invariant signatures, CIS Report No. 9419, Computer Science Department, Technion, Israel (December 1994).
25. L. Van Gool, T. Moons, D. Ungureanu and A. Oosterlinck, The characterization and detection of skewed symmetry, *Comput. Vision Image Understanding* **61**, 138–150 (1995).
26. T. Glauser and H. Bunke, Edge length ratios: An affine invariant shape representation for recognition with occlusions, *Proc. Eleventh ICPR*, Hague (1992).
27. L. Morin, P. Brand and R. Mohr, Indexing with projective invariants, *Proc. SSPR94 Workshop*, Nahariya (1994).
28. R. Lenz and P. Meer, Point configuration invariants under simultaneous projective and permutation transformations, *Pattern Recognition* **27**, 1523–1532 (1994).

About the Author — ALFRED M. BRUCKESTEIN was born in Transylvania, Romania, on 24 January 1954. He received the B.Sc. and M.Sc. degrees in Electrical Engineering, from the Technion, Israel Institute of Technology, in 1977 and 1980, respectively, and the Ph.D. degree in Electrical Engineering from Stanford University, Stanford, California, in 1984. From October 1984, he has been with the Technion, Haifa, Israel, where he is a Professor of Computer Science. He is a frequent visitor at Bell Laboratories, Murray Hill, New Jersey (where he presently spends a sabbatical). His research interests are in computer vision, pattern recognition, image processing, and computer graphics. He has also done work in estimation theory, signal processing, algorithmic aspects of inverse scattering, point processes and mathematical models in neurophysiology. Professor Bruckstein is a member of SIAM, MAA and AMS.

About the Author — DORON SHAKED graduated from the Electrical and Computer Engineering Department of the Ben Gurion University in Beer Sheva, Israel, in 1988. M.Sc. and D.Sc. from the Electrical Engineering Department of the Technion, in Haifa, Israel, in 1991 and 1995, respectively. He was Ollendorf Fellow (1991), and received the Wolf Prize for an excellent student (1994). Currently, he is with Hewlett Packard Israel Science Center. His research interests include: computer vision, pattern recognition, shape analysis, axial shape representation and thinning algorithms, sequential decision theory, and color printing.